The American Journal of Pathology, Vol. 181, No. 6, December 2012

http://dx.doi.org/10.1016/j.ajpath.2012.08.016

Cell Injury, Repair, Aging, and Apoptosis

DNA Methylation Plasticity of Human Adipose-Derived Stem Cells in Lineage Commitment

María Berdasco,* Consolación Melguizo,† Jose Prados,† Antonio Gómez,* Miguel Alaminos,‡ Miguel A. Pujana,§ Miguel Lopez,* Fernando Setien,* Raul Ortiz,† Inma Zafra,† Antonia Aranega,† and Manel Esteller*¶‖

From the Cancer Epigenetics Group, Cancer Epigenetics and Biology Program, and the Cancer Systems Biology Group,§ Translational Research Laboratory, Catalan Institute of Oncology, Bellvitge Biomedical Biomedical Research Institute, Barcelona; the Institute of Biopathology and Regenerative Medicine,† School of Medicine, and the Department of Histology,‡ University of Granada, Granada; the Department of Physiological Sciences II,¶ School of Medicine, University of Barcelona, Barcelona; and the Catalan Institution for Research and Advanced Studies,‖ Barcelona, Spain*

Adult stem cells have an enormous potential for clinical use in regenerative medicine that avoids many of the drawbacks characteristic of embryonic stem cells and induced pluripotent stem cells. In this context, easily obtainable human adipose-derived stem cells offer an interesting option for future strategies in regenerative medicine. However, little is known about their repertoire of differentiation capacities, how closely they resemble the target primary tissues, and the potential safety issues associated with their use. DNA methylation is one of the most widely recognized epigenetic factors involved in cellular identity, prompting us to consider how the analyses of 27,578 CpG sites in the genome of these cells under different conditions reflect their different natural history. We show that human adipose-derived stem cells generate myogenic and osteogenic lineages that share much of the DNA methylation landscape characteristic of primary myocytes and osteocytes. Most important, adult stem cells and *in vitro*–generated myocytes and osteocytes display a significantly different DNA methylome from that observed in transformed cells from these tissue types, such as rhabdomyosarcoma and osteosarcoma. These results suggest that the plasticity of the DNA methylation patterns plays an important role in lineage commitment of adult stem cells and that it could be used for clinical purposes as a biomarker of efficient and safely differentiated cells. *(Am J Pathol 2012, 181:2079–2093; http://dx.doi.org/10.1016/j.ajpath.2012.08.016)*

Human adipose-derived stem cells (hASCs) refer to the plastic-adherent and multipotent cell population isolated from collagenase digests of adipose tissue. Although the differentiation capacity of hASCs was initially thought to be limited to their tissue of origin, recent data have demonstrated that multipotent stem cells retain a broad differentiation potential. hASCs can be induced to differentiate along several mesenchymal tissue lineages, including adipocytes, osteoblasts, myocytes, and chondrocytes.[1–3] hASCs also differentiate into neuron-like cells expressing neuronal markers.[4–6] The differentiation ability of hASCs has generated interest because of their potential clinical use in regenerative medicine.[7] They meet the criteria for application in regenerative medicine in the following ways: i) they are found in abundant quantities, ii) they can be collected and harvested by a minimal invasive procedure, iii) they can be differentiated into multiple cell lineage pathways in a reproducible manner, and iv) they can be safely and effectively transplanted into an autologous or allogenic host.[8]

Gene expression potential in stem cell differentiation is regulated by epigenetic processes that confer a specific chromatin conformation on the genome, of which post-translational modifications of histone tails and CpG dinucleotide methylation are the best characterized. Much attention

Supported by grants from the European Research Council (Advanced EPINORC), the Spanish Health Ministry (PI08-1345), the Spanish Science and Innovation Ministry (SAF2011-22803), the Fundació La Marató de TV3 (111430/31), the European Cooperation in Science and Technology (COST TD09/05), and the Health Department of the Catalan Government (Generalitat de Catalunya). M.E. is a Catalan Institution for Research and Advanced Studies Research Professor.

Accepted for publication August 23, 2012.

Supplemental material for this article can be found at *http://ajp.amjpathol.org* or at *http://dx.doi.org/10.1016/j.ajpath.2012.08.016*.

Address reprint requests to Manel Esteller, M.D., Ph.D., Cancer Epigenetics and Biology Program, Bellvitge Biomedical Research Institute, Floor 3, Duran i Reynals Hospital, Av. Gran Via 199-203, 08908 L'Hospitalet, Barcelona, Catalonia, Spain. E-mail: mesteller@idibell.cat.

is being paid to the effects of CpG methylation on stemness and differentiation. The first evidence came from the observation that genes important for the maintenance of pluripotency in embryonic stem cells (ESCs), such as *OCT4* and *NANOG*, are usually hypomethylated when activated, whereas they become hypermethylated during differentiation.[9,10] High-throughput strategies for genome-wide DNA profiling demonstrate that human ESCs have a unique CpG methylation signature, which, in combination with histone modifications, drives stem cell differentiation by restricting the developmental potential of progenitor cells.[11–13] The epigenetic control of pluripotency is not restricted to the classic pluripotency-related genes, because it has been recently described that hypermethylation of tissue-specific genes also controls the reprogramming ability of somatic cells into pluripotent cells.[14] In contrast with the wide-ranging information obtained from ESCs, the role of CpG methylation in regulating differentiation of adult multipotent stem cells has been less extensively examined.[15] Adult stem cells of different origin (eg, adipose tissue, bone marrow, or hematopoietic progenitor cells) display a range of differentiation potentials in mesodermal, endodermal, and ectodermal tissues,[16] and strong methylation of lineage-specification promoters restricts the ability of adult stem cells of different origin to differentiate.[17] For example, methylation of endothelial cell–specific genes (*CD31* and *CD144*) has been described in freshly isolated hASCs, but not in differentiated cells, after endothelial stimulation.[18] Preliminary genome-wide approaches, including gene expression, CpG methylation, histone marks, and microRNA (miRNA) analysis,[19] allow a connection to be established between changes in the epigenetic signature and progression from pluripotent to multipotent cells, highlighting the existence of specific epigenetic profiles associated with each degree of differentiation potential. The epigenetic control of stem cell differentiation is also reinforced by several *in vitro* experimental studies with chromatin-modifying drugs. Specific epigenetic treatments can alter the potential of pluripotent and multipotent stem cells to differentiate into several lineages.[15] For example, the use of DNA demethylation treatment (5-aza-2′-deoxycytidine) promotes differentiation of multipotent cells into cardiac myogenic cells[20] and drives the osteogenic differentiation of mesenchymal stem cells.[21]

Despite the knowledge about how to govern stem cell differentiation, we still lack information about the degree of similarity between stem cell derivatives and their normal primary counterparts. The success of stem cell differentiation is usually addressed by expression of a set of differentiation markers and loss of pluripotency-related genes. In addition, to achieve appropriate quality and control of these cells, we must also ensure the integrity of the epigenome and avoid inappropriate gene expression in transplanting cells or tumorigenesis. Herein, we have performed a high-throughput analysis using methylation arrays of well-characterized and defined populations of hASCs before and after *in vitro* induction of osteogenic and myogenic differentiation. Most important, the CpG methylation profile of these cells has been compared with those obtained from normal primary cells and tumor samples. Overall, our results demonstrate that hASCs generate osteogenic and myogenic lineages that resemble the DNA methylome of primary tissues, but do not present the epigenetic hallmarks of cancer cells. These findings suggest that the profile of CpG methylation could be used as a biomarker of efficient and safe cell identity after stem cell reprogramming.

Materials and Methods

Human Adipose-Derived Stem Cell Populations

hASCs were established from the adipose tissue of patients aged 30 to 55 years. Samples were obtained by minimally invasive liposuction procedures. Donors previously gave their written informed consent, in accordance with the guidelines of the Ethics Committee of the Nuestra Señora de la Salud Hospital (Granada, Spain). hASC lines were established as previously described.[22] Briefly, lipoaspirates were digested with 0.075% collagenase type I (Invitrogen SA, Barcelona, Spain) prepared in PBS containing 1% bovine serum albumin for 1 hour at 37°C with constant shaking, followed by filtration through a 100-μm filter. After washing with PBS, cells were treated with erythrocyte lysis buffer. Resultant cells were cultivated at 1000 cells/cm^2 in Dulbecco's modified Eagle's medium (DMEM) supplemented with 10% fetal bovine serum (FBS). Cultures were washed with buffer for 24 to 48 hours after plating to remove unattached cells, and then refed with fresh medium. Only cells in passage 5 or 6 were used in these experiments. Positive and negative surface markers for hASCs, defined by the International Society for Cellular Therapy, were studied by fluorescence-activated cell sorting (FACSCanto II Cytometer; BD Biosciences, San Jose, CA). Cells were removed from culture using a nonenzymatic cell dissociation solution (Sigma-Aldrich, Madrid, Spain) and washed with PBS. The following antibodies were used: CD73, CD90, CD105, CD45, CD34, and CD133 (BD Biosciences). Approximately 2 $\times$ 10^5 cells were incubated with primary antibody directly coupled to fluorescein isothiocyanate, allophycocyanin, or phycoerythrin for 15 minutes in the dark at room temperature.

In Vitro *Differentiation*

hASCs were differentiated to osteogenic and myogenic lineages by *in vitro* induction using specific culture medium.[23] Osteogenesis was induced in the presence of DMEM with 10% FBS, 0.1 mol/L dexamethasone, 10 mmol/L β-glycerophosphate, and 50 g/mL ascorbic acid-2-phosphate. After 28 days, the culture medium was removed and cells were washed with PBS and processed. Calcium deposition was visualized by alizarin red staining and confirmed by X-ray microanalysis of cultured cells under the scanning electron microscope (SEM), following the method of Kim et al.[24] In addition, RT-PCR analysis using mRNA obtained from total cells incubated in osteogenic medium was performed to determine gene expression of osteonectin, osteopontin, and osteocalcin. Myogenic induction of hASCs was performed in the presence of DMEM with 10% FBS, 50 mol/L hydrocortisone, and 5% horse serum. After 42 days, the degree of myogenic differentiation was analyzed by immunofluorescence using monoclonal antibodies against α-sarcomeric actin (clone 5C5; Sigma-Aldrich), α-sarcomeric

actinin (clone EA-53; Sigma-Aldrich), and troponin T-C (clone C-19; Santa Cruz Biotechnology, Inc., Santa Cruz, CA). In addition, RT-PCR analysis using mRNA of these cells was used to determine gene expression of desmin, myosin-1, and myogenic differentiation 1. A complementary study to determine the regression of osteogenic and myogenic differentiation was performed by analyzing the induced cells after removing the culture medium supplemented with the differentiation agents over 14 and 20 days for osteogenic and myogenic induction, respectively. The RT-PCR primers and annealing temperatures (Tm) used were as follows: desmin (Tm = 51°C), 5′-GGTGGAGGTGCTCACTAACC-3′ (antisense) and 5′-TGTTGTCCTGGTAGCCACTG-3′ (antisense); myosin-1 (Tm = 51°C), 5′-TGTGAATGCCAAATGTGCTT-3′ (sense) and 5′-GTGGAGCTGGGTATCCTTGA-3′ (antisense); myogenic differentiation 1 (Tm = 52°C), 5′-AAGCGC-CATCTCTTGAGGTA-3′ (sense) and 5′-GCGCCTTTATTTT-GATCACC-3′ (antisense); osteocalcin (Tm = 56°C), 5′-GCTCTAGAATGGCCCTCACACTC-3′ (sense) and 5′-GCGATATCCTAGACCGGGCCGTAG-3′ (antisense); osteonectin (Tm = 53°C), 5′-TGTGGGAGCTAATCCTGTCC-3′ (sense) and 5′-TCAGGACGTTCTTGAGCCAGT-3′ (antisense); and osteopontin (Tm = 50°C), 5′-GCTCTAGAAT-GAGAATTGCACTG-3′ (sense) and 5′-GTCAATGGAGTC-CTGGCTGT-3′ (antisense).

Cancer Cell Lines and Primary Tissues

The human rhabdomyosarcoma (RD and TE.32.7) and osteosarcoma (MG-63) cell lines were obtained from ATCC (Rockland, MD). Cell lines were maintained in monolayer cultures at 37°C in an atmosphere containing 5% CO_2, with DMEM supplemented with 10% FBS. Normal primary cells were obtained from biopsy specimens of the rectus abdominis muscle (myocytes) and ribs (osteocytes) under histological validation, and the samples were stored at −80°. All samples were obtained in accordance with the guidelines of the Ethics Committee of the Bio-Health Research Foundation of Eastern Andalusia (Granada, Spain).

DNA Methylation Profiling Using Universal Bead Arrays

DNA from adipose-derived stem cells, *in vitro*–differentiated cells, cancer cell lines, and primary tissues was isolated by applying the QIAamp DNA Mini Kit (Qiagen, Iberia, Spain). Microarray-based DNA methylation profiling was performed with the HumanMethylation2 BeadChip Infinium Methylation Arrays (Illumina, Inc.) on a total of five adipose-derived stem cells, six *in vitro*–differentiated cells, three normal primary tissues, and three cancer cell lines. The panel was designed to compare the DNA methylation status of each group of samples, which allow 27,578 CpG loci covering 14,495 genes at single-nucleotide resolution to be interrogated by typing bisulfite-converted DNA. The sequences included in the panel were derived from the well-annotated National Cancer for Biotechnology Information consensus coding sequence (CCDS) database (Genome Build 36) and were supplemented by >1000 cancer-related genes described in the literature. The probe content was enriched to include >150 well-established cancer genes known to show differential methylation patterns. The methylation array content also targeted the promoter regions of 110 miRNA genes.

Methylation arrays were then performed. First, 1 μg of genomic DNA was bisulfite converted using the CpGenomicTM DNA Modification Kit (Intergen Company, Purchase, NY). After sodium bisulfite treatment, the remaining assay steps used Infinium technology (Illumina Inc, San Diego, CA), previously described for single-nucleotide polymorphism genotyping[25] with manufacturers' supplied reagents and conditions. A thermocycling program with a short denaturation step included for bisulfite conversion (16 cycles at 95°C for 30 seconds, followed by 50°C for 1 hour) was performed to improve the bisulfite conversion efficiency. After bisulfite conversion, each sample was whole-genome amplified and enzymatically fragmented. The bisulfite-converted whole-genome amplified DNA samples were purified and applied to the BeadChips (Illumina Inc, San Diego, CA). During hybridization, the whole-genome amplified DNA molecules annealed to locus-specific DNA oligomers linked to individual bead types. The two bead types corresponded to each CpG locus: one to the methylated and the other to the unmethylated state. Allele-specific primer annealing was followed by single-base extension using dinitrophenyl- and biotin-labeled dNTPs. Both bead types for the same CpG locus incorporated the same type of labeled nucleotide, determined by the base preceding the interrogated cytosine in the CpG locus, and could, therefore, be detected in the same color channel. After extension, the array was fluorescently stained and scanned, and the intensities of the unmethylated and methylated bead types were measured.

DNA methylation values, described as β values, were recorded for each locus in each sample via BeadStudio software (Illumina Inc). The DNA methylation β value is a continuous variable between 0 (completely unmethylated) and 1 (completely methylated), and represents the ratio of the intensity of the methylated bead type/combined locus intensity. The DNA methylation microarray data are freely available for download from the National Cancer for Biotechnology Information Gene Expression Omnibus (*http://www.ncbi.nlm.nih.gov/geo*; accession number GSE33896).

Hierarchical Cluster Analysis and Definition of CpG Methylation Differences

Hierarchical clustering was performed on all of the studied samples using the Cluster Analysis tool of the BeadStudio software version 3.2 (Illumina Inc). CpGs included in the analysis had to meet two criteria: a false-discovery rate of <0.01 and not being located on the X chromosome (to avoid a sex-specific bias). To investigate the methylation profiles, we first excluded the CpGs with a coefficient of variation of >0.25 for samples to discount intrasample variation among those of the same category. Averages were calculated from the resulting sequences.

Differentially methylated CpG sites were determined calculating the differences in average β values between groups. A threshold of >0.20 change in average β values and a false-discovery rate of <0.01 in an analysis of variance test, adjusted for multiple testing, was applied to assign significant differentially methylated sites.[26]

Bisulfite Genomic Sequencing of Multiple Clones

We determined the CpG island methylation status of the selected genes by PCR analysis of bisulfite-modified genomic DNA, which induces the chemical conversion of unmethylated, but not methylated, cytosine to uracil. After PCR and cloning, 10 clones of each sequence and sample were automatically sequenced to determine their degree of methylation. Primer sequences and annealing temperatures used were as follows: CD79B (Tm = 59°C), 5′-GGGGTAAGTATAGATAGAGGGGA-3′ (sense) and 5′-AATAAAAACAAACCCCACAAAC-3′ (antisense); CDKL1 (Tm = 59°C), 5′-CAAAATCATCTTCTAATTCCAAAA-3′ (sense) and 5′-TTAGTTTTTTGAGTTGTTGGGA-3′ (antisense); PIWI-like 2 (PIWIL2; Tm = 58°C), 5′-GTAGGTTGGGTTTTTGTTTAAGT-3′ (sense) and 5′-TAACCAAAAACAAAACCCC-3′ (antisense); receptor-type tyrosine-protein phosphatase S (PTPRS; Tm = 58°C), 5′-TGTGGGGGAGATATTTTAATTT-3′ (sense) and 5′-CCTTCTACTACACAACCTCCAA-3′ (antisense); serum amyloid A1 (SAA1; Tm = 58°C), 5′-GTTTTGAGTGAGGTTTTGTTGT-3′ (sense) and 5′-ATTTTCCCCAATTTATCAAATC-3′ (antisense); solute carrier family 44 member 2 (SLC44A2; Tm = 58°C), 5′-GGGTTTTTTAGTTTGGGTAGTT-3′ (sense) and 5′-TATTCTCTCAAAACCCCCTC-3′ (antisense); and transmembrane channel-like 8 (TMC8; Tm = 62°C), 5′-ACTCCRACACCCCAAAAA-3′ (sense) and 5′-GTGTGTTTTTTTGAGAGTTGGAG-3′ (antisense).

Expression Microarrays

For the expression microarray experiment in hASCs and *in vitro* differentiated cells, total RNA was prepared using TRIzol (Invitrogen, Carlsbad, CA) and further purified using RNeasy columns (Qiagen, GmbH, Germany), according to the manufacturers' instructions. The integrity of RNA was monitored by both Byoanalyzer (Agilent, Santa Clara, CA) and spectrometric measurement. Biotinylated target RNA was prepared from 200 ng of total RNA using the Affymetrix protocol (Affymetrix, Santa Clara, CA). Briefly, double-stranded cDNA was prepared from the RNA template using the Ambion WT Expression kit, following manufacturer's instructions. The resulting complementary RNA target was randomly fragmented using uracil DNA glycosylase and apurinic/apyrimidic endonuclease 1, labeled with the terminal transferase (WT Terminal Labeling kit; Affymetrix) and hybridized on the Human Gene 1.1 ST 16-array (Affymetrix). The hybridization reactions were processed and scanned according to the standard GeneTitan (Affymetrix) protocols. All arrays were globally scaled to a target intensity value of 100 and then the scaling factor, background, noise, and percentage present were calculated according to the Command Console (AGCC 2.0) and Expression Console (EE 1.1) software (Affymetrix, High Wycombe, UK). All resulting data sets were filtered using the absolute call metric (present or absent) using Microsoft Access (Microsoft Corporation, Redmond, WA). The resulting values represent the transcript abundance (absolute value) following the Affymetrix statistical procedure. Three biological replicates were obtained for each ASC sample, and *in vitro*–differentiated cells were analyzed in duplicate. The DNA expression microarray data are freely available for download from NCBI Gene Expression Omnibus (*http://www.ncbi.nlm.nih.gov/geo*; accession number GSE37329).

Transcriptome Data Analysis

To identify all genes or probe sets whose expression was significantly different between control adipose-derived stem cells and each one of the two differentiated cell types (osteogenis or myogenic differentiation), we used the following approach under R statistical language: the raw data coming from the Affymetrix Human Gene 1.1 ST platform were preprocessed and normalized using the Affymetrix package (background subtraction and quantile normalization), then the differential expression was assessed using a linear model procedure (limma package).[27] The differentially expressed genes with at least 20% expression increase (fold-change >1.2) or 20% expression decrease (fold-change <0.8) after induction were selected, and the resultant *P* values were adjusted for multiple testing using the Benjamini and Hochberg correction procedure.

Gene Ontology Analysis

Gene ontology (GO) analysis of the selected genes was performed using the Bioconductor package GOstats (Bioconductor, Boston, MA).[28] The set of selected genes was tested for enrichment of any GO category, and the *P* values for multiple testing were adjusted using the Benjamini and Hochberg correction procedure.

Comparisons between Differentially Methylated and Differentially Expressed Genes

Because of the fact that the genes differentially expressed and methylated are not the same for myogenic and osteogenic lineages, we conducted a difference between two lists using their functional profiles. We used squared euclidean distance to quantify the difference between profiles[26] and calculate *P* values.

RT-qPCR Expression Analysis

Total RNA was prepared from all samples using TRIzol (Invitrogen, Carlsbad) and further purified using RNeasy columns (Qiagen, GmbH), according to the manufacturers' instructions. For quantitative RT-PCR assays, 2 μg of total RNA was converted to cDNA with the ThermoScriptTM RT-PCR System (Invitrogen) using oligo-dT as primer. PCR amplifications were performed as follows: 0.20 μg of

cDNA and 5 pmol of each primer and SYBR Green PCR Master Mix (Applied Biosystems, Foster City, CA). Three measurements were analyzed using a Prism 7700 Sequence Detection (Applied Biosystems) instrument. Quantitative RT-PCR (RT-qPCR) primer sequences were as follows: *PIWIL2*, 5′-GTGGGTTGAGCTCGGTCTT-3′ (sense) and 5′-GGACGGGCTGTAGAGAACAC-3′ (antisense); *PTPRS*, 5′-ACTCGGCCAACTACACCTG-3′ (sense) and 5′-GGCTGTGTTCTCAGTCACCA-3′ (antisense); and *SAA1*, 5′-AGCCGAAGCTTCTTTTCGTT-3′ (sense) and 5′-GCCGATGTAATTGGCTTCTC-3′ (antisense). Primer sequences for osteogenic differentiation markers were as follows: osteopontin, 5′-CGCAGACCT-GACATCCAGTA-3′ (sense) and 5′-ATTCAACTCCT-CGCTTTCCA-3′ (antisense); and alkaline phosphatase, 5′-TGAAATATGCCCTGGAGCTT-3′ (sense) and 5′-TCACT-GTGGAGACACCCATC-3′ (antisense). Primer sequences for myogenic differentiation markers were as follows: desmin, 5′-TGATGGAATACCGACACCAG-3′ (sense) and 5′-GCCTCATCAGGGAATCGTTA-3′ (antisense); and myocyte enhancer factor 2A, 5′-TGATGCGGAATCATA-AAATCG-3′ (sense) and 5′-GGCTGGTCACTGGAACT-GTG-3′ (antisense). Three independent measurements were performed for each condition, and the SD was calculated.

RNA Interference

Three small-interfering RNA (siRNA) duplexes that recognized three different sequences against the *PIWIL2* gene were designed. The siRNA primers were for the following regions: 1, 5′-GTGGCCACAAGCTTCTAAACTTCAA-GAGAGTTTAGAAGCTTGTGGCCATTTTTTACGCGT-3′ (sense) and 5′-ACGCGTAAAAAATGGCCACAAGCTTCTA-AACTCTCTTGAAGTTTAGAAGCTTGTGGCCAC-3′ (antisense); 2, 5′-GTGCTAATCTGGTACGCAAGTTCAA-GAGACTTGCGTACCAGATTAGCATTTTTTACGCGT-3′ (sense) and 5′-ACGCGTAAAAAATGCTAATCTGGTACG-CAAGTCTCTTGAACTTGCGTACCAGATTAGCAC-3′ (antisense); and 3, 5′-GCCTACAAGTGCTATGGTACTTCAA-GAGAGTACCATAGCACTTGTAGGTTTTTTACGCGT-3′ (sense) and 5′-ACGCGTAAAAAACCTACAAGTGCTATG-GTACTCTCTTGAAGTACCATAGCACTTGTAGGC-3′ (antisense). As a negative control, the following scramble primers (a target with any complementary human coding regions) were used: 5′-GCGCAGAACAAATTCGTCC-ATTCAAGAGATGGACGAATTTGTTCTGCGTTTTTTAC-GCGT-3′ (sense) and 5′-ACGCGTAAAAAACGCA-GAACAAATTCGTCCATCTCTTGAATGGACGAA-TTTGTTCTGCGC-3′ (antisense). The previously mentioned siRNA oligonucleotides were cloned into a pLVX-shRNA2 lentivirus vector (Clontech, Mountain View, CA), following supplier's instructions. Green clones expressing fluorescent ZsGreen1 protein were selected for further experiments. Silencing of *PIWIL2* expression was confirmed by protein blotting.

Western Blot Analysis

For Western blot analysis, we collected cells by centrifugation, washed cell pellets twice with phosphate buffered saline (PBS) buffer, and extracted total proteins with Laemmli buffer. Protein separation was performed on a 7.5% SDS-PAGE gel. Fractions were transferred to a nitrocellulose membrane with a 45-μm pore size (Immobilon PTM or Millipore filter; Millipore Ibérica, Madrid, Spain), blocked in 5% milk PBS with 0.1% Tween-20, and immunoprobed with the respective primary antibodies. We used the corresponding horseradish enhanced chemiluminescence (ECLTM) peroxidase–conjugated antibody to IgG (GE Healthcare; Amersham, Pittsburgh, PA) at 1:3000 dilution as a secondary antibody. Signals were detected with an ECLTM Western blot detection reagent (GE Healthcare; Amersham, Pittsburgh, PA). Primary antibody was used at 1:1000 dilution (ab85084; Abcam, Cambridge, UK).

Results

Generation of Osteogenic and Myogenic Lineages from Human Adipose-Derived Stem Cells

hASCs were obtained from lipoaspirates according to the criteria established by the International Society for Cellular Therapy for defining mesenchymal stem cells.[29] hASCs grew as adherent spindle-shaped fibroblastoid cells and were positive for CD73, CD90, and CD105 surface markers, and negative for CD34, CD45, and CD133 (Figure 1A). hASCs were successfully differentiated into osteogenic and myogenic lineages. Calcium deposition was visualized by alizarin red staining in cells after 28 days of osteogenic induction (Figure 1B). Energy-dispersive X-ray analysis in the SEM of these differentiated cells confirmed the presence of this chemical element (Figure 1B). Determination by RT-PCR of osteonectin, osteopontin, and osteocalcin gene expression was consistent with the osteogenic differentiation process (Figure 1B). For the myogenic differentiation of hASCs, the expression of established muscle-specific markers was determined by immunofluorescence and RT-PCR. As shown in Figure 1C, differentiated hASCs were strongly stained for troponin T-C, α-sarcomeric actin, and actinin. Differentiation of hASCs into myogenic precursor cells was confirmed by the expression of transcription factors, such as myogenic differentiation 1, and structural proteins, such as myosin-1 and desmin (Figure 1C).

DNA Methylation Changes Associated with Osteogenic and Myogenic Differentiation of Human Adipose-Derived Stem Cells

We analyzed the DNA methylation status of 27,578 CpG sites of the human genome (Infinium 27K Illumina arrays) in hASCs taken from different donors ($n = 4$) compared with hASC-derived osteocytes (known as *in vitro* osteocytes; $n = 3$) or hASC-derived myocytes (known as *in vitro* myocytes; $n = 3$). Unsupervised scatterplots of all of

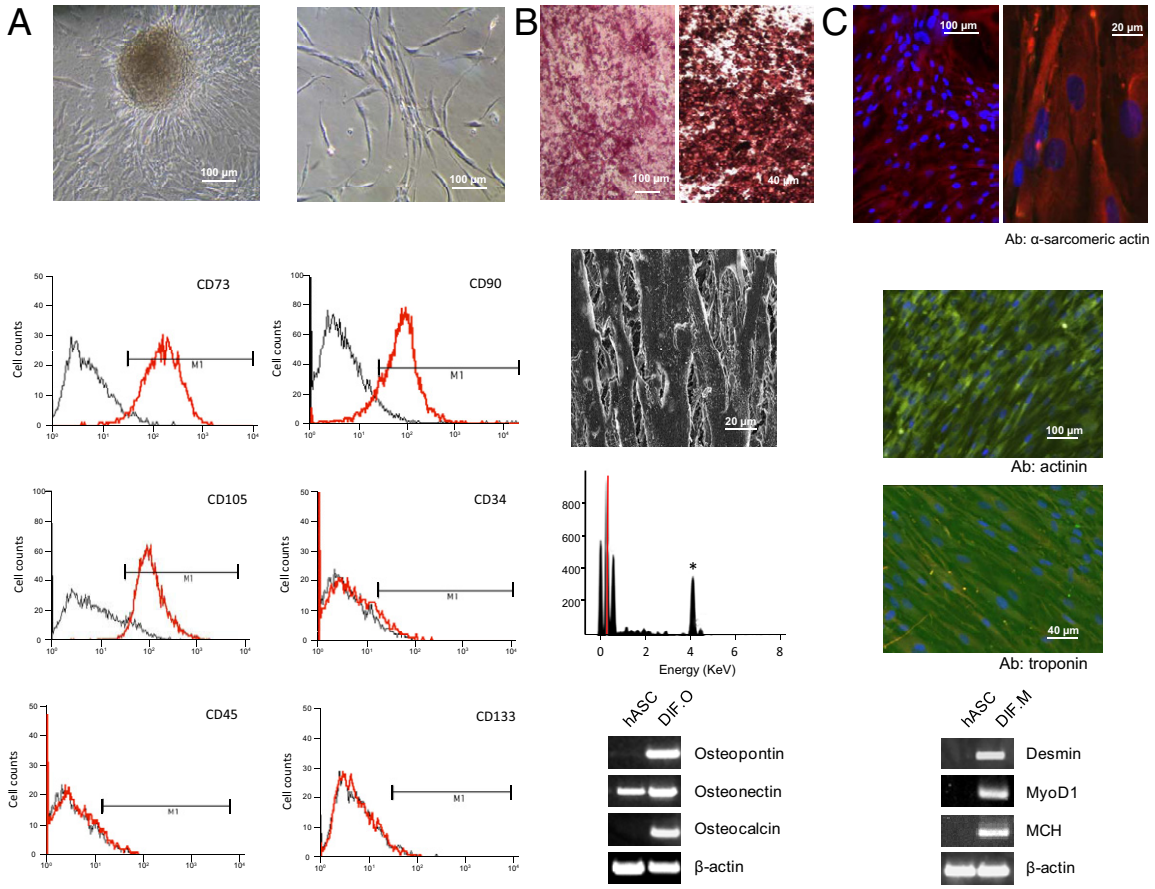

Figure 1. Characterization of hASCs and induction of differentiation. **A:** Characterization of hASCs. **Top panels:** hASCs grow as a monolayer adhering to the surface and form colonies. **Bottom panel:** Immunophenotypic characterization of hASCs by FACScan analysis showing high levels of CD73, CD90, and CD105 molecules. In contrast, the cells are negative for CD34, CD45, and CD133. **B:** Osteogenic differentiation from hASC-derived cells after 28 days was monitored as follows: staining with alizarine [**top panel**, original magnification, ×10 (**left**), ×40 (**right**)], calcium detection by SEM–X-ray microanalysis with chemical element peaks shown in the graph (**middle panels**), and analysis of the expression levels of well-known markers of osteogenic differentiation by RT-PCR (**bottom panel**). The **asterisk** indicates calcium peaks obtained in SEM–X-ray microanalysis. **C: Top** and **middle panels**, myogenic differentiation from hASC-derived cells after 42 days was monitored by staining with antibodies to muscle-specific proteins, such as α-sarcomeric actin [original magnification, ×10 (**left**), ×40 (**right**)], actinin (original magnification, ×10), and troponin (original magnification, ×20). **Bottom panel**, analysis of the expression levels of well-known markers of myogenic differentiation by RT-PCR. DIF.O, *in vitro* osteocytes; DIF.M, *in vitro* myocytes; MCH, myosin-1; MyoD, myogenic differentiation.

the CpG probes contained in the microarray of the hASC samples and their corresponding osteogenic or myogenic differentiated cells revealed a high degree of similarity in their CpG methylation patterns (Figure 2A). To search for specific changes in the methylation status of particular CpGs during both types of differentiation, we used a threshold-based method using three replicates for each sample and a >20% CpG methylation β value as the cutoff. We obtained 108 differentially methylated CpG dinucleotides between hASCs and *in vitro*–differentiated cells: there were 85 differentially methylated CpG sites in hASCs versus the myogenic lineage (see Supplemental Table S1 at *http://ajp.amjpathol.org*), whereas 23 CpG sites changed their methylation value after induction of osteogenic differentiation in hASCs (see Supplemental Table S2 at *http://ajp.amjpathol.org*), which enabled both types of samples to be classified into distinct clustering arms in the hierarchical analysis (Figure 2B). Among the 108 CpG sites, the CpG methylation shift most often occurred in promoter-associated CpG islands [71 (66%) of 108 CpGs], which most frequently consisted of a methylation gain in the differentiated cells [84 (78%) of 108 CpGs]. To address the biological role of the differentially methylated CpGs after osteogenic or myogenic differentiation, we identified GO terms enriched among these CpGs. The GO analysis of groups of genes differentially methylated demonstrated enrichments of gene functions associated with regulation functions ($P < 0.05$) (see Supplemental Table S3 at *http://ajp.amjpathol.org*).

We further validated the observed DNA methylation microarray data in our differentiation model from hASCs using bisulfite genomic sequencing of multiple clones in differentially methylated candidate genes. We selected three genes that represented a committed osteogenic pathway (*SAA1*),[30] an established neuromuscular route (*PTPRS*),[31] and a gene marker of stemness (*PIWIL2*).[32] These three genes also represented the two differential CpG contents: *PTPRS* and *PIWIL2* contain a 5′ end–associated CpG island, whereas the *SAA1* minimal promoter is a CpG-poor region. Bisulfite genomic sequencing showed dense hypermethylation of the *PTPRS* promoter CpG island in hASCs that became demethylated on the

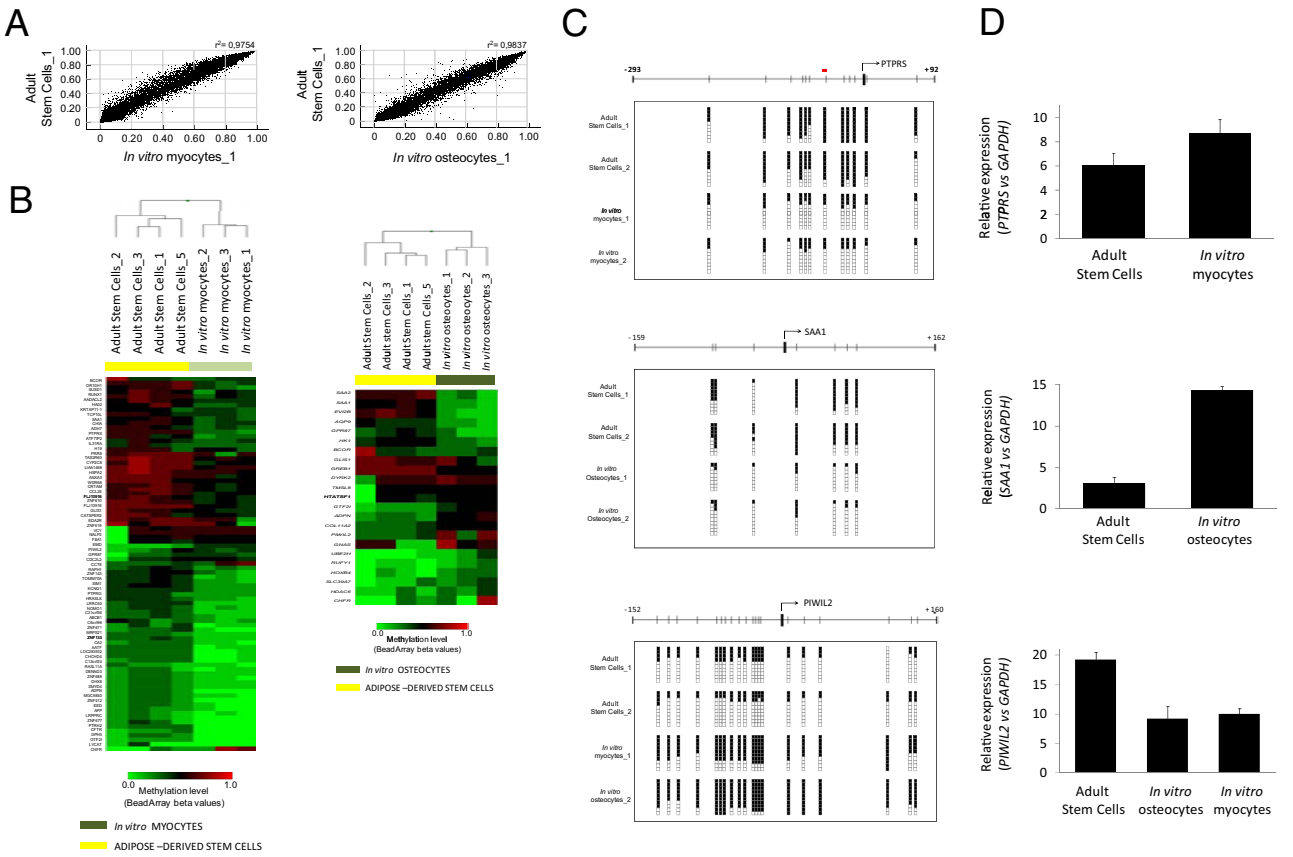

Figure 2. Specific promoter methylation events during *in vitro* differentiation of adipose-derived stem cells. **A:** Two-dimensional scatterplots of Infinium methylation values in a representative adipose-derived stem cell sample versus an *in vitro*–differentiated cell sample for each lineage. **B:** Supervised clustering using the most significantly differentially methylated CpGs after myogenic and osteogenic differentiation of adipose-derived stem cells. **C:** Analysis of promoter CpG methylation status of differentially methylated genes after induction of differentiation by bisulfite genomic sequencing. Schematic depiction of the *PTPRS*, *SAA1*, and *PIWIL2* CpG dinucleotides around the transcription start site (**long black arrow**). CpG dinucleotides are represented as short vertical lines. Results of bisulfite genomic sequencing of 10 individual clones are shown. The presence of a methylated or unmethylated cytosine is indicated by a black or white square, respectively. **D:** Expression levels of each PTPRS, SAA1, and PIWIL2 mRNA relative to glyceraldehyde-3-phosphate dehydrogenase (GAPDH), detected by RT-qPCR.

induction of myogenic differentiation (Figure 2C). Likewise, in the other differentiation pathway, the *SAA1* 5′-end CpG-poor region was heavily methylated in hASCs and became hypomethylated on the induction of osteogenic differentiation (Figure 2C). In an opposite manner to these genes, the 5′-regulatory CpG island of *PIWIL2* was essentially unmethylated in hASCs, but it became densely methylated when the cell became committed to both myogenic and osteogenic pathways (Figure 2C).

The relevance of the described CpG methylation shifts was reinforced by the study of the expression dynamics of the previously mentioned genes. *PTPRS* and *SAA1*, showing a hypermethylated 5′-end region in hASCs (a CpG island for *PTPRS* and a CpG-poor region for *SAA1*), both demonstrated an absence of their transcripts in the mesenchymal stem cells, as determined by quantitative real-time RT-PCR (Figure 2D). The CpG hypomethylation events on differentiation previously described were associated with a gain of expression of *PTPRS* and *SAA1* in myogenic and osteogenic differentiation, respectively (Figure 2D). The expression profiles of *PIWIL2* occurred in the opposite manner to that of *PTPRS* and *SAA1*, and they fit the corresponding DNA methylation changes: the *PIWIL2* transcript was present in the mesenchymal unmethylated stem cells, but it was repressed on the induction of both lineages in association with the gain of *PIWIL2* CpG island hypermethylation (Figure 2D).

To establish a functional consequence of the changes in DNA methylation during differentiation, we analyzed gene expression profiles using the Affymetrix Human Gene 1.1 ST Array. We compared the expression of hASCs ($n = 2$) with the induced differentiated cells corresponding to myogenic ($n = 2$) and osteogenic ($n = 2$) lineages, and we identified a set of genes differentially expressed before and after differentiation (see Supplemental Table S4 and Supplemental Table S5 at *http://ajp.amjpathol.org*). Because the genes differentially expressed and methylated were not exactly the same, we conducted a difference between two lists using their functional profiles using squared euclidean distance to quantify the difference between profiles. The *P* values associated with distance values are >0.05 (0.4616 and 0.6966 for myogenic and osteogenic lineages, respectively), suggesting that no significant statistical differences could be established between methylation and expression groups (ie, the two functional profiles in both cases were equivalent).

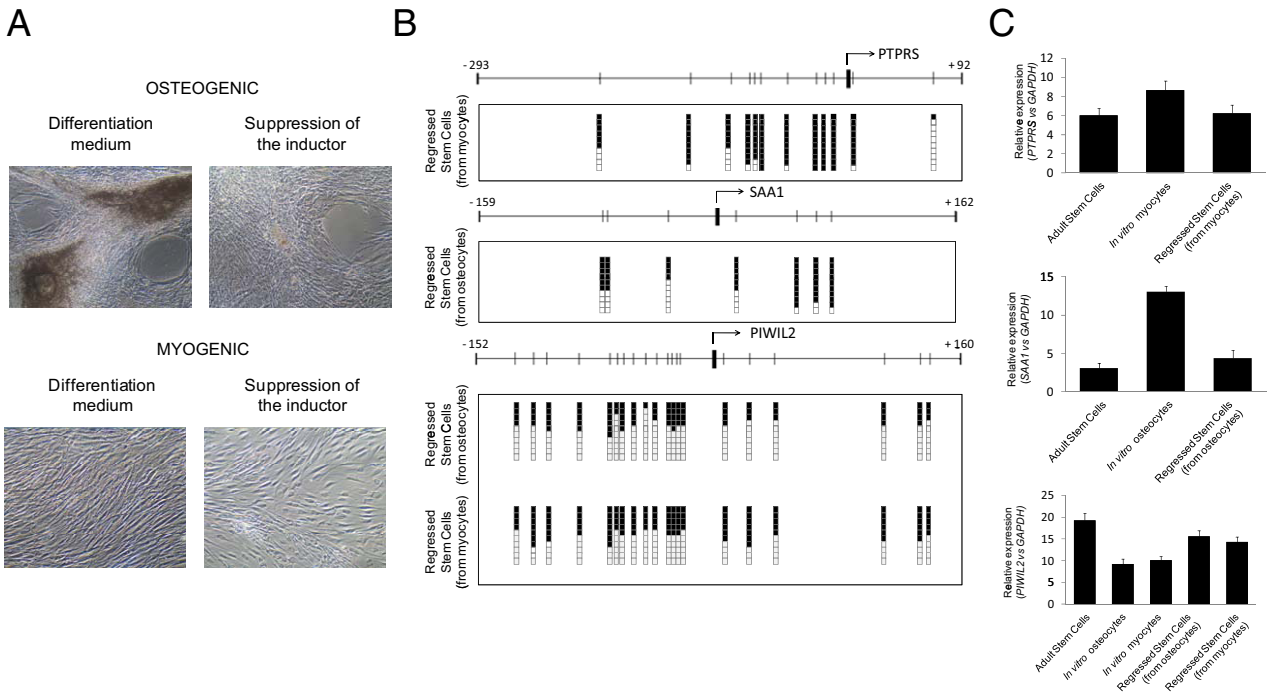

Figure 3. Differentiated cells deprived of the induction factor reacquire multipotent stem cell phenotype. **A:** Adipose-derived stem cell differentiated for osteogenic and myogenic lineage showing significant morphological changes after 14 and 20 days in culture, respectively, without induction factors. **B:** Bisulfite genomic sequencing of the promoter region of *PTPRS, SAA1*, and *PIWIL2* genes in regressed stem cells. CpG dinucleotides are represented as short vertical lines. The results of bisulfite genomic sequencing of 10 individual clones are shown. The presence of a methylated or unmethylated cytosine is indicated by a black or white square, respectively. **C:** The expression levels of PTPRS, SAA1, and PIWIL2 mRNA relative to glyceraldehyde-3-phosphate dehydrogenase (GAPDH) detected by RT-qPCR in regressed cells.

Plasticity of the Epigenetic Setting of Human Adipose-Derived Stem Cells—Restoration of DNA Methylation Patterns on Regression of the Differentiation Process

Unlike the constrained genetic landscape, the epigenetic profiles of cells and tissues adapted quickly to changes in the surrounding microenvironment.[33] We examined how closely the observed DNA methylation patterns were associated with the osteogenic and myogenic lineage and whether a return to the adult stem cell stage was linked to a shift in DNA methylation profiles. Therefore, we evaluated the effect of deprivation of the induction factors for osteogenic and myogenic differentiation in the culture media. As shown in Figure 3A, osteogenic and myogenic cells cultured for 15 to 20 days in the absence of differentiation agents lost the phenotypic features of the lineage (eg, normal muscle typical cell alignment) and recovered the morphological characteristics of the original hASCs.

Most important, the regression to an adult stem cell phenotype of the *in vitro*–differentiated cells was associated with a complete reversion of the DNA methylation patterns (Figure 3B). If bisulfite genomic sequencing revealed an unmethylated *PTPRS* promoter CpG island in myogenic cells, it became hypermethylated on the deprivation of the differentiating factor (Figure 3B). Similarly, in the other differentiation pathway, the *SAA1* 5′-end CpG-poor region that was unmethylated in induced osteogenic differentiation became hypermethylated on the regression to adult stem cell status (Figure 3B). In contrast, the 5′-regulatory CpG island of *PIWIL2* that was densely methylated in both *in vitro*–differentiated lineages underwent hypomethylated changes when the cells were deprived of the myogenic and osteogenic commitment factors in their growth media (Figure 3B). The importance of CpG methylation dynamics was supported by the study of the expression changes of the described genes. *PTPRS* and *SAA1*, with an unmethylated 5′-end region in the *in vitro*–induced myogenic and osteogenic cells, both demonstrated a loss of their transcripts on regression to mesenchymal stem cell status, as determined by quantitative real-time PCR (Figure 3C). The hypermethylation of *SAA1* in regressed cells did not correspond with the low expression levels in ASCs. The poor-CpG promoter content of *SAA1* could justify this absence of linear correlation between expression and CpG methylation. The opposite correlation was observed for *PIWIL2* transcription: on withdrawal of the differentiating factor from the two lineages, the adult stem cell phenotypic cells recovered the expression of the *PIWIL2* transcript (Figure 3C), in association with the previously described *PIWIL2* CpG island hypomethylation events.

Once we demonstrated that *PIWIL2* epigenetic silencing was associated with entrance into a differentiation program, we assayed the effect of abrogation of *PIWIL2* expression by siRNA in our model. We stably silenced *PIWIL2* in adipose-derived stem cells by using three different duplexes that recognized three different sequences against the *PIWIL2* gene sequence. *PIWIL2*

expression was monitored by RT-PCR and Western blot analysis (see Supplemental Figure S1 at *http://ajp.amjpathol.org*). We observed that *PIWIL2* silencing facilitated cellular differentiation. Specific markers for myogenic differentiation appeared after 21 days of induction in *PIWIL2*-depleted cells, instead of 42 days in ASCs expressing *PIWIL2* (see Supplemental Figure S1 at *http://ajp.amjpathol.org*), whereas osteogenic markers in si-*PIWIL2* cells appeared at day 20, instead of day 28 (see Supplemental Figure S1 at *http://ajp.amjpathol.org*).

Distinct DNA Methylation Profile of Osteogenic and Myogenic Lineages Derived from Human Adipose Stem Cells and Primary Osteocytes and Myocytes

To fulfill the promise of novel biomedical therapies based on adult stem cells, a critical issue in the field was the analysis of how closely related the *in vitro*–generated differentiated cells were to the targeted primary tissue.[34,35] To address this question, we compared the DNA methylation status of 27,578 CpG sites of the human genome (Infinium 27K Illumina arrays) in the *in vitro*–obtained osteogenic and myogenic lineages derived from human adipose stem cells with that of freshly isolated primary normal osteocytes and myocytes obtained from healthy donors. Unsupervised scatterplots using all of the CpG probes contained in the microarray revealed significant differences in their CpG methylation patterns (Figure 4A). To search for specific changes in the methylation status of particular CpGs during *in vitro* compared with natural differentiation, we used a threshold-based method involving three replicates for each sample and a >20% CpG methylation β value as a cutoff. This identified 4712 differentially methylated CpGs: there were 2313 differentially methylated CpG dinucleotides in the myogenic lineage relative to the hASCs (see Supplemental Table S6 at *http://ajp.amjpathol.org*), whereas 2399 CpG sites changed their methylation value after induction of osteogenic differentiation in hASCs (see Supplemental Table S7 at *http://ajp.amjpathol.org*), which enabled both types of samples to be classified into distinct clustering arms in the hierarchical analysis (Figure 4B). Among the total 4712 CpG sites, the CpG methylation shifts occurred in CpG-poor promoters [3103 CpGs (66%)] and promoter-associated CpG islands [1609 CpGs (34%)]. The most common difference was a lower rate of CpG methylation in the *in vitro*–differentiated cells than in the primary tissues [2807 (60%) of 4712 CpGs] (Figure 4C). The type of CpG methylation differences observed between *in vitro*–differentiated and primary cells, according to the lineage, are shown in Supplemental Figure S2 (available at *http://ajp.amjpathol.org*). In addition, differentially methylated genes between *in vitro*–differentiated cells (derived from stem cells) and *in vivo*–differentiated cells (from donors) were mostly enriched for GO terms associated with signal transduction and system development. An enrichment of defense and immune response ($P < 0.05$) was also described in both myogenic and osteogenic lineages (see Supplemental Table S3 at *http://ajp.amjpathol.org*).

We further validated the observed DNA methylation microarray data in *in vitro*–differentiated cells from adult stem cells compared with primary tissues by bisulfite genomic sequencing of multiple clones in differentially methylated candidate genes. We selected four genes that represented the two observed DNA methylation scenarios. The *SLC44A2* and *CDKL1* genes had a 5′-end regulatory region that was unmethylated in the respective osteogenic and myogenic lineages (Figure 4D), but these regions were densely methylated in their normal counterparts (Figure 4D). On the other hand, the *CD79B* and *TMC8* genes showed highly methylated 5′ regions around their transcription start sites in the stem cell–differentiated osteocytes and myocytes (Figure 4D), but the primary osteocytes and myocytes obtained from the volunteers were unmethylated for the described sequences (Figure 4D).

Distinct DNA Methylation Profile of Osteogenic and Myogenic Lineages Derived from Human Adipose Stem Cells and Osteosarcoma and Rhabdomyosarcoma Cells

To establish a possible clinical use for the *in vitro*–differentiated cells originating from adult stem cells, it was also extremely important to ensure that the obtained lineages had not acquired a tumorigenic potential[36–38] or that the original adipose stem cells were not themselves carriers of cancer-prone DNA methylation features.

To address this first question, we analyzed the DNA methylation status of 27,578 CpG sites of the human genome (Infinium 27K Illumina arrays) in the *in vitro*–obtained osteogenic and myogenic lineages derived from human adipose stem cells compared with osteosarcoma and rhabdomyosarcoma cells, respectively. Unsupervised scatterplots of all of the CpG probes contained in the microarray of the osteogenic or myogenic differentiated lineages derived from the adult stem samples revealed significant differences in the CpG methylation patterns compared with those of the corresponding transformed cells (Figure 5A). To search for specific changes in the methylation status of particular CpGs during *in vitro* differentiation that could be shared with tumor cells, we used a threshold-based method using three replicates for each sample and a >20% CpG methylation β value as a cutoff. By using this approach, we obtained 7007 differentially methylated CpG sites between the *in vitro*–differentiated lineages and the transformed cells. A total of 2166 CpG dinucleotides were differentially methylated in the myogenic lineage compared with the rhabdomyosarcoma cells (see Supplemental Table S8 at *http://ajp.amjpathol.org*), whereas 4841 CpG sites had a different methylation value in *in vitro*–differentiated osteocytes and osteosarcoma cells (see Supplemental Table S9 at *http://ajp.amjpathol.org*). This enabled both types of samples to be classified into distinct clustering arms in the hierarchical analysis (Figure 5B). Among all 7007 CpG sites, the CpG methylation shifts occurred in promoter-associated CpG islands [4161 CpGs (59%)] and CpG-poor promoters [2846 CpGs (41%)]. However, there was clear

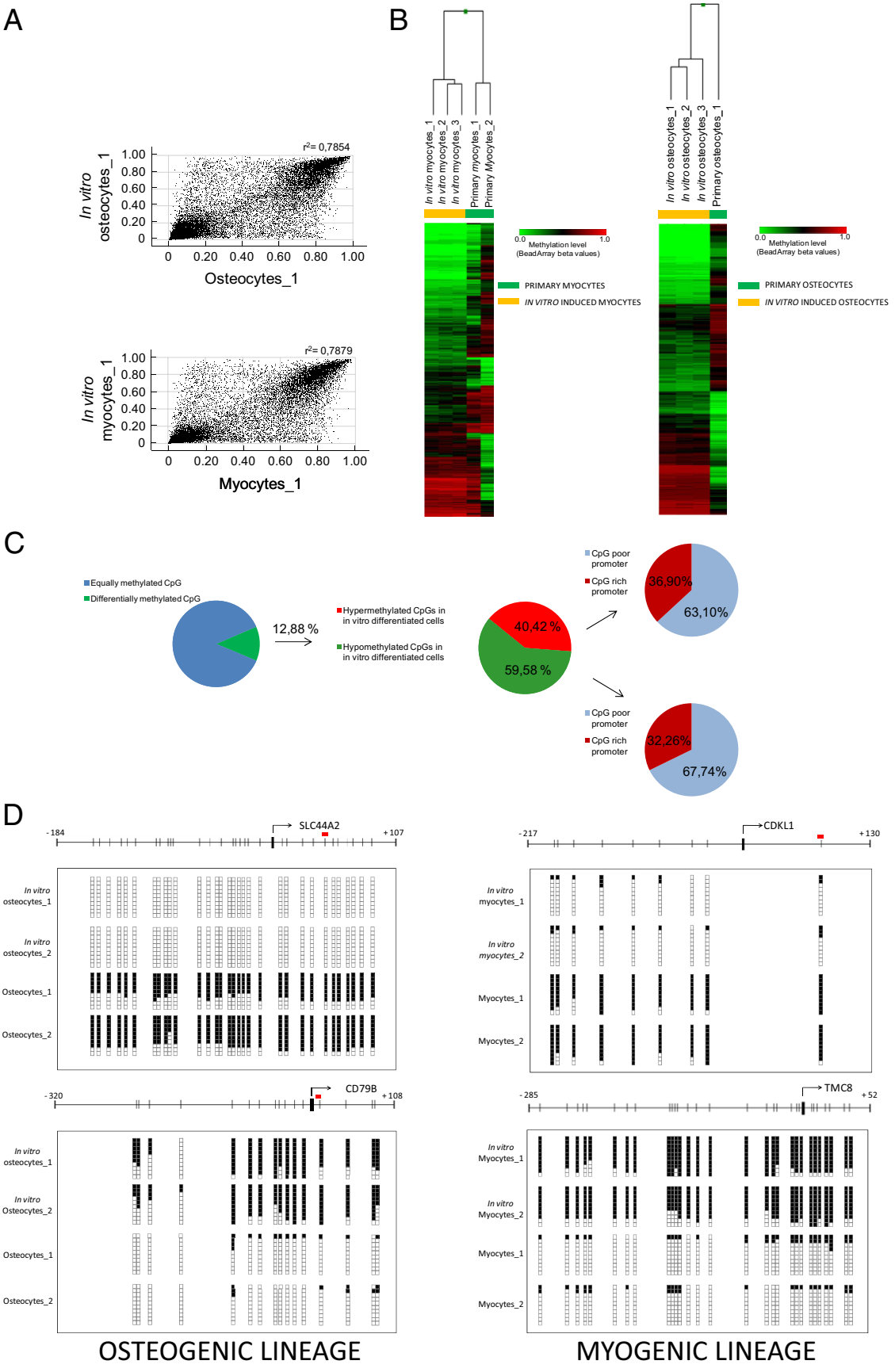
A
In vitro osteocytes_1
Osteocytes_1
r²= 0,7854
In vitro myocytes_1
Myocytes_1
r²= 0,7879
B
In vitro myocytes_1
In vitro myocytes_2
In vitro myocytes_3
Primary myocytes_1
Primary Myocytes_2
Methylation level (BeadArray beta values)
PRIMARY MYOCYTES
IN VITRO INDUCED MYOCYTES
In vitro osteocytes_1
In vitro osteocytes_2
In vitro osteocytes_3
Primary osteocytes_1
PRIMARY OSTEOCYTES
IN VITRO INDUCED OSTEOCYTES
C
Equally methylated CpG
Differentially methylated CpG
12,88 %
Hypermethylated CpGs in in vitro differentiated cells
Hypomethylated CpGs in in vitro differentiated cells
40,42 %
59,58 %
CpG poor promoter
CpG rich promoter
36,90%
63,10%
32,26%
67,74%
D
SLC44A2
CDKL1
CD79B
TMC8
OSTEOGENIC LINEAGE
MYOGENIC LINEAGE

enrichment of methylation changes in CpG-rich promoters associated with hypermethylation in tumorigenic samples for the myogenic and osteogenic lineages (Fisher's exact test, two-tailed $P < 0.0001$). The most common difference was a higher frequency of CpG methylation in transformed cells than in *in vitro*–differentiated cells [5096 (73%) of 7007 CpGs] (Figure 5C).

Finally, we compared the DNA methylation profiles of the original adipose stem cells and of the myogenic and osteogenic cancer cells to exclude the existence of significant DNA methylation changes associated with cellular transformation[39,40] in the adult stem cells. Unsupervised scatterplots using all of the CpG probes contained in the microarray revealed significant differences in their CpG methylation patterns (Figure 5D). We found 7823 CpG sites to be differentially methylated in the adult stem cells and the transformed cells. A total of 4024 CpG dinucleotides were differentially methylated in hASCs compared with rhabdomyosarcoma cells (see Supplemental Table S10 at *http://ajp.amjpathol.org*), whereas 3799 CpG sites had a different methylation value in adult stem cells and osteosarcoma cells (see Supplemental Table S11 at *http://ajp.amjpathol.org*). This enabled both types of samples to be classified into distinct clustering arms in the hierarchical analysis (Figure 5E). Among all 7823 CpG sites, the CpG methylation shifts occurred in promoter-associated CpG islands [4300 CpGs (55%)] and CpG-poor promoters [3523 CpGs (45%)]. Again, we found significant enrichment of gain of methylation in tumor samples specifically in CpG-rich promoters (Fisher's exact test, two-tailed $P < 0.0001$). The most common difference was a higher frequency of CpG methylation in the transformed cells than in *in vitro*–differentiated cells [6531 (83%) of 7823 CpGs] (Figure 5F).

Referring to the functional clustering of differentially methylated genes involving cancer cells, the GO analysis demonstrated enrichments of genes mostly involved in regulation of cellular processes, signal transduction, and development ($P < 0.05$) (see Supplemental Table S3 at *http://ajp.amjpathol.org*).

Overall, our data showed that it is possible to generate myogenic and osteogenic lineages from easily obtainable adipose stem cells that, according to a comprehensive DNA methylation analysis of 27,578 CpG sites, resemble the corresponding primary differentiated tissues and did not present the DNA methylation hallmarks of cancer cells. This supported their putative use for translational and clinical purposes.

Discussion

The conversion of human pluripotent ESCs into differentiated somatic cells is believed to involve only small changes in DNA methylation at promoter regions.[9,10,13,41,42] For instance, 8% of unmethylated CpGs in hESCs became methylated after differentiation to neural precursors, whereas 2% of methylated CpGs in hESCs lose methylation in neural precursors.[41] Similar results were described for adult stem cell differentiation: 80% of the promoter hypermethylation in differentiated adipocytes (from adipose-derived stem cells) and myocytes (from skeletal muscle–derived stem cells) was also present in nondifferentiated cells. If we consider the small proportion of sequences with differential methylation, the silencing of specific pluripotency-related genes, such as *OCT4* or *NANOG*,[9] by *de novo* promoter methylation is well-known. Our results also demonstrate that stem cell differentiation from hASCs involves changes in the methylation patterns of a few genes.

The epigenetic silencing of *PIWIL2* in committed cells in osteogenic and myogenic lineages is of particular note. The PIWI/Ago family is required for stem cell maintenance.[25] PIWIL2, also known as MILI proteins, interacts with the epigenetic mechanism by controlling the RNA interference mechanism.[43,44] PIWI proteins bind to 24 to 31 nucleotide PIWI-interacting RNAs and regulate germ line development, stem cell maintenance, epigenetic regulation, and transposition.[45–47] DNA methylation of *Oct4* and *Nanog* promoters could be a mechanism for preventing aberrant reactivation of pluripotency and for minimizing the risk of dedifferentiation.[48] Our results suggest that *PIWIL2* epigenetic control must also be important for maintaining the multipotent ability in adipose-derived stem cells.

Silencing of stemness-related genes is one critical step in stem cell commitment, but we must also account for the gain of expression of differentiation genes. Specific demethylation events are frequently linked to gene activation on somatic differentiation, such as the reactivation of tissue-specific genes (eg, *Lrrtm2*) coupled to loss of promoter methylation in neural differentiation from mouse ESCs.[13] We found that PTPRS, a protein with a role in neuronal and lymphoblastoid differentiation,[49,50] and SAA1, which is involved in osteogenic differentiation,[23] behaved in the same way in hASC-derived differentiation. It remains uncertain how DNA methylation could contribute to tissue-specific gene expression and differentiation. There are a few studies investigating the link between DNA methylation of CpG-rich promoters and tissue-specific gene expression, and a small, but signif-

Figure 4. DNA methylation profile of *in vitro*–differentiated cells and the corresponding normal primary tissues. **A:** Two-dimensional scatterplots of Infinium methylation values in a representative sample from *in vivo* normal primary tissue (from rib and muscle) versus each *in vitro*–differentiated cell. **B:** Supervised cluster analysis and heat map showing the differential groups of CpGs according to their DNA methylation profile in all analyzed samples. HumanMethylation27 BeadChip Infinium Methylation Arrays are performed in normal primary tissues from ribs and muscle (green bar) and in *in vitro* myocytes and osteocytes (yellow bar). Methylation levels vary from fully methylated (red) to fully unmethylated (green). **C:** Percentage of differentially methylated CpG sites in *in vitro* differentiated cells compared with primary tissues. The genomic distribution in CpG-rich or CpG-poor promoters of the differentially methylated CpGs is also indicated. **D:** Promoter CpG methylation status of differentially methylated genes by bisulfite sequencing. Schematic depiction of the *SLC44A2*, *CD79B*, *CDKL1*, and *TMC8* CpG islands around the transcription start site (**long black arrow**). The location of the probe included in the methylation array is indicated by a red bar. CpG dinucleotides are represented as short vertical lines. The results of bisulfite genomic sequencing of 10 individual clones are shown. The presence of a methylated or unmethylated cytosine is indicated by a black or white square, respectively.

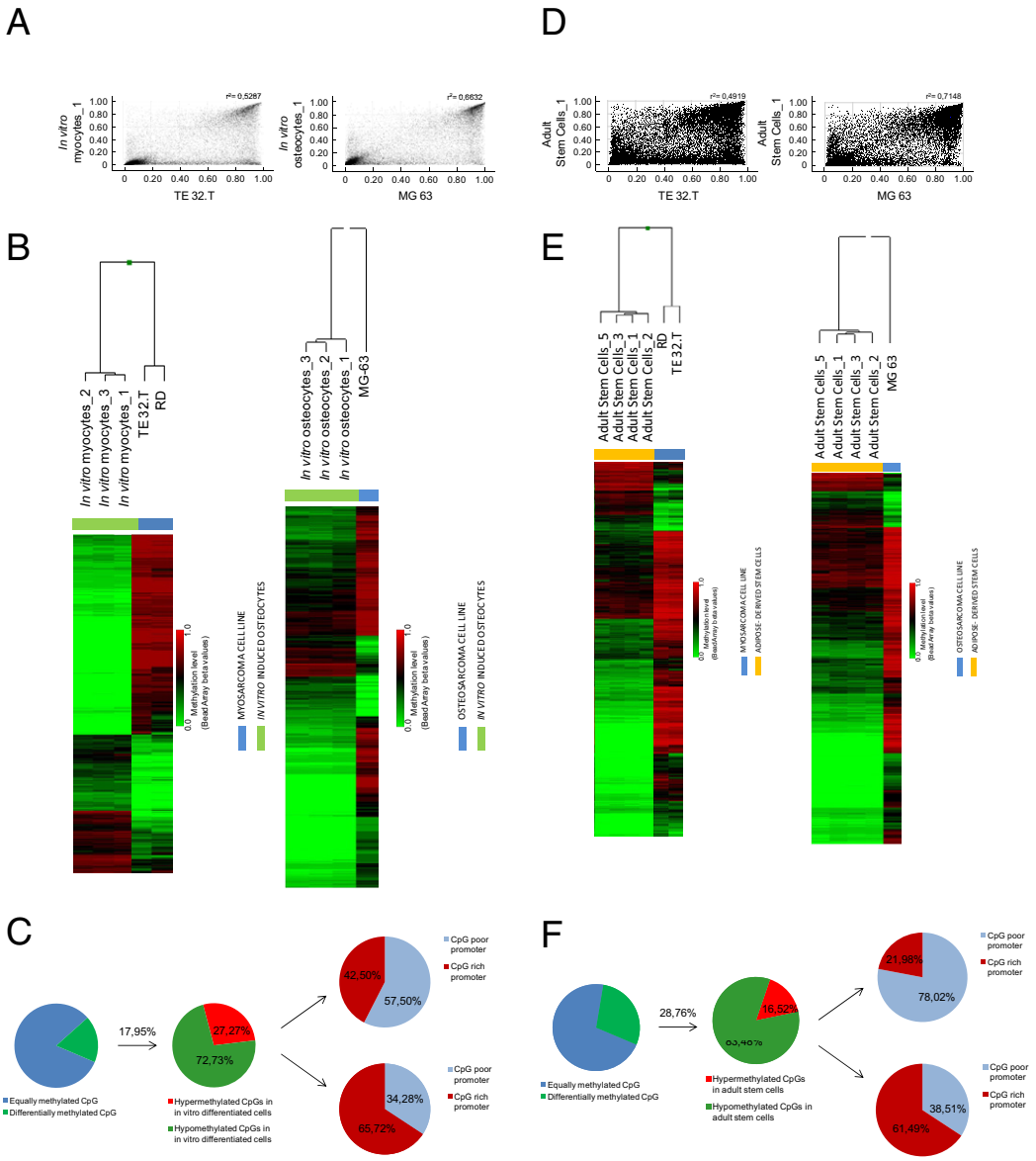

Figure 5. A comparison of CpG methylation profiles in stem cells, stem cell derivatives, and cancer cell lines. **A:** Two-dimensional scatterplots of Infinium methylation values in one representative sample of *in vitro*–differentiated cells (**left panel,** myogenic induction; **right panel,** osteogenic induction) versus their corresponding cancer cell lines. **B:** Supervised cluster analysis and heat map displaying the differential groups of CpGs according to their DNA methylation profile in *in vitro*–differentiated cells (green bar) and cancer cell lines (blue bar). **C:** Percentage of differentially methylated CpG sites in *in vitro*–differentiated cells with respect to cancer cell lines. The genomic distribution in CpG-rich or CpG-poor promoters of the differentially methylated CpGs is also indicated. **D:** Two-dimensional scatterplots of Infinium methylation values in one representative sample of an adult stem cell versus a myosarcoma cell line (**left panel**) and an osteosarcoma cell line (**right panel**). **E:** Supervised cluster analysis and heat map displaying the differential groups of CpGs according to their DNA methylation profile in adult stem cells (yellow bar) and cancer cell lines (blue bar). **F:** Percentage of differentially methylated CpG sites in adult stem cells with respect to cancer cell lines. The genomic distribution in CpG-rich or CpG-poor promoters of the differentially methylated CpGs is also indicated. RD and TE 32.T, rhabdomyosarcoma cell lines; MG-63, osteosarcoma cell line.

icant, proportion of genes have been identified as differentially methylated among cell types.[51–53] The expression of the human *MASPIN* (*SERPINB5*) gene is limited to certain types of epithelial cells, but no detectable amounts of the gene are found in skin fibroblasts, lymphocytes, bone marrow, heart, or kidney.[52] Consistent with this finding, other genes, such as *rSPHK1* and *hSLC6A8*, showed promoter hypermethylation associated with gene silencing in specific tissues.[51,54] Furthermore, recent studies identified tissue-specific differentially methylated regions located far away from the promoters that could be subject to changes in methylation during development.[55,56]

Our results suggest that DNA methylation profiles could be used as a biomarker of appropriate differentiation. However, the results also reinforce the dynamic nature of epigenetic regulation under certain environmental signals, as was demonstrated by the reversion of the DNA methylation levels of *PTPRS*, *SAA1*, and *PIWIL2* genes in the deprivation experiments. Are some genes (or chromosomal regions) more epigenetically stable than others? A recent article linked an epigenetic mechanism to the ability of human

adult stem cells to initiate osteogenic differentiation. Fan et al[57] described how a mutation in BCL6 corepressor (BCOR), a transcriptional repressor of the activating protein 2 AP2α, induces osteogenesis through histone modifications. Thus, we revised the methylation levels of BCOR in our 27K Illumina assays, and confirmed that BCOR is highly methylated in normal bone (methylation value, 0.95) but hemimethylated in *in vitro* osteocytes (methylation value, 0.44). This partial epigenetic reprogramming of hASC-derived cells could also explain the possibility of regression in the first steps of differentiation, as we demonstrated in our deprivation experiments. Indeed, under certain experimental conditions, a mature cell can be converted into a pluripotent state by the *in vitro* application of a defined set of transcription factors controlled by promoter hypermethylation, generating induced pluripotent stem cells.[58–60] Furthermore, the recent finding that somatic cells can be reprogrammed to pluripotency merely by overexpressing certain ESC-specific miRNAs that target differentiation genes,[61] together with the role of specific miRNAs in cell differentiation (ie, miR-1 and miR-206 in myogenic differentiation),[62] suggests that epigenetic control plays a far more important role in differentiation than previously suspected.

Finally, one critical step in the development of stem cell–based therapies in regenerative medicine is the ability to manipulate stem cells into differentiated cells, ensuring cell identity after reprogramming and minimizing the risk of tumorigenesis. In contrast to the well-addressed genomic instability in ESC derivatives,[63] reports of malignant transformation of adult stem cells are scarce, but spontaneous oncogenic transformation has been described in some long-term cultured stem cells, which is one of the requisites for transplantation purposes.[64,65] A complex two-step model has recently been proposed that involves alterations in cell cycle, mitochondrial metabolism, and DNA repair, together with oncogene expression and silencing of tumor-suppressor genes, by which a mesenchymal stem cell becomes a tumor cell.[66] In addition, clonal chromosomal aberrations may also arise transiently in early passage of hASC cultures.[67]

The question arises as to whether DNA methylation is altered during large-scale culture of hASCs. Only a few DNA methylation–dependent genes are affected by the passage number of hASCs under specific culture conditions. Dahl et al[68] did not find any significant change in the DNA methylation status of specific promoters. They compared DNA methylation in bone marrow stem cells with freshly isolated and cultured hASCs and showed that most genes unmethylated in both bone marrow stem cells and hASCs during early passage are also unmethylated in uncultured hASCs. Herein, we also assessed the risk of tumorigenesis of adipose-derived stem cells and their derivatives by comparing their methylation patterns with those obtained from tumor samples (rhabdomyosarcoma and osteosarcoma cell lines). Aberrant DNA methylation patterns, including hypermethylation of tumor suppressor genes, are one of the main hallmarks of cancer cells.[69,70] Our methylation array, which is enriched in CpGs representing CpG islands on promoter regions, allows the hypermethylation profiles of stem cells and cancer cells to be examined. Our results suggest that the genome-wide hypermethylation profile of hASCs and derived differentiated cells strongly differs from that obtained in cancer cell lines, indicating that the tumorigenic properties of specific stem cell populations[66] could be generated by CpG methylation–independent mechanisms.

Overall, our data demonstrate that myogenic and osteogenic cells derived from adipose stem cells acquire part of the DNA methylation setting of the primary corresponding differentiated tissues, but neither of them features the DNA methylation profiles of transformed cells. Most notably, our results highlight the necessity of performing appropriate molecular tests to ensure the integrity of the epigenome in any candidate cell line or tissue intended for use in regenerative therapy.

References

1. Zuk PA, Zhu M, Ashjian P, De Ugarte DA, Huang JI, Mizuno H, Alfonso ZC, Fraser JK, Benhaim P, Hedrick MH: Multilineage cells from human adipose tissue: implications for cell-based therapies. Tissue Eng 2001, 7:211–228
2. Halvorsen YD, Bond A, Sen A, Franklin DM, Lea-Currie YR, Sujkowski D, Ellis PN, Wilkison WO, Gimble JM: Thiazolidinediones and glucocorticoids synergistically induce differentiation of human adipose tissue stromal cells: biochemical, cellular, and molecular analysis. Metabolism 2001, 50:407–413
3. Erickson GR, Gimble JM, Franklin DM, Rice HE, Awad H, Guilak F: Chondrogenic potential of adipose tissue-derived stromal cells in vitro and in vivo. Biochem Biophys Res Commun 2002, 290:763–769
4. Kang SK, Putnam LA, Ylostalo J, Popescu IR, Dufour J, Belousov A, Bunnell BA: Neurogenesis of Rhesus adipose stromal cells. J Cell Sci 2004, 117(Pt 18):4289–4299
5. Safford KM, Safford SD, Gimble JM, Shetty AK, Rice HE: Characterization of neuronal/glial differentiation of murine adipose-derived adult stromal cells. Exp Neurol 2004, 187:319–328
6. Trottier V, Marceau-Fortier G, Germain L, Vincent C, Fradette J: IFATS collection: using human adipose-derived stem/stromal cells for the production of new skin substitutes. Stem Cells 2008, 26:2713–2723
7. Zuk PA: The adipose-derived stem cell: looking back and looking ahead. Mol Biol Cell 2010, 21:1783–1787
8. Gimble JM, Katz AJ, Bunnell BA: Adipose-derived stem cells for regenerative medicine. Circ Res 2007, 100:1249–1260
9. Lagarkova MA, Volchkov PY, Lyakisheva AV, Philonenko ES, Kiselev SL: Diverse epigenetic profile of novel human embryonic stem cell lines. Cell Cycle 2006, 5:416–420
10. Fouse SD, Shen Y, Pellegrini M, Cole S, Meissner A, Van Neste L, Jaenisch R, Fan G: Promoter CpG methylation contributes to ES cell gene regulation in parallel with Oct4/Nanog, PcG complex, and histone H3 K4/K27 trimethylation. Cell Stem Cell 2008, 2:160–169
11. Bibikova M, Chudin E, Wu B, Zhou L, Garcia EW, Liu Y, Shin S, Plaia TW, Auerbach JM, Arking DE, Gonzalez R, Crook J, Davidson B, Schulz TC, Robins A, Khanna A, Sartipy P, Hyllner J, Vanguri P, Savant-Bhonsale S, Smith AK, Chakravarti A, Maitra A, Rao M, Barker DL, Loring JF, Fan JB: Human embryonic stem cells have a unique epigenetic signature. Genome Res 2006, 16:1075–1083
12. Calvanese V, Horrillo A, Hmadcha A, Suarez-Alvarez B, Fernandez AF, Lara E, Casado S, Menendez P, Bueno C, Garcia-Castro J, Rubio R, Lapunzina P, Alaminos M, Borghese L, Terstegge S, Harrison NJ, Moore HD, Brüstle O, Lopez-Larrea C, Andrews PW, Soria B, Esteller M, Fraga MF: Cancer genes hypermethylated in human embryonic stem cells. PLoS One 2008, 3:e3294
13. Mohn F, Weber M, Rebhan M, Roloff TC, Richter J, Stadler MB, Bibel M, Schübeler D: Lineage-specific polycomb targets and de novo DNA methylation define restriction and potential of neuronal progenitors. Mol Cell 2008, 30:755–766
14. Barrero MJ, Berdasco M, Paramonov I, Bilic J, Vitaloni M, Esteller M, Izpisua Belmonte JC: DNA hypermethylation in somatic cells correlates with higher reprogramming efficiency. Stem Cells 2012, 30:1696–1702

15. Berdasco M, Esteller M: DNA methylation in stem cell renewal and multipotency. Stem Cell Res Ther 2011, 2:42
16. Kern S, Eichler H, Stoeve J, Klüter H, Bieback K: Comparative analysis of mesenchymal stem cells from bone marrow, umbilical cord blood, or adipose tissue. Stem Cells 2006, 24:1294–1301
17. Sørensen AL, Timoskainen S, West FD, Vekterud K, Boquest AC, Ahrlund-Richter L, Stice SL, Collas P: Lineage-specific promoter DNA methylation patterns segregate adult progenitor cell types. Stem Cells Dev 2010, 19:1257–1266
18. Boquest AC, Noer A, Sørensen AL, Vekterud K, Collas P: CpG methylation profiles of endothelial cell-specific gene promoter regions in adipose tissue stem cells suggest limited differentiation potential toward the endothelial cell lineage. Stem Cells 2007, 25:852–861
19. Aranda P, Agirre X, Ballestar E, Andreu EJ, Román-Gómez J, Prieto I, Martín-Subero JI, Cigudosa JC, Siebert R, Esteller M, Prosper F: Epigenetic signatures associated with different levels of differentiation potential in human stem cells. PLoS One 2009, 4:e7809
20. Choi SC, Yoon J, Shim WJ: 5-Azacytidine induces cardiac differentiation of P19 embryonic stem cells. Exp Mol Med 2004, 36:515–523
21. Zhou GS, Zhang XL, Wu JP, Zhang RP, Xiang LX, Dai LC, Shao JZ: 5-Azacytidine facilitates osteogenic gene expression and differentiation of mesenchymal stem cells by alteration in DNA methylation. Cytotechnology 2009, 60:11–22
22. Bunnell BA, Flaat M, Gagliardi C, Patel B, Ripoll C: Adipose-derived stem cells: isolation, expansion and differentiation. Methods 2008, 45:115–120
23. Zuk PA, Zhu M, Mizuno H, Huang J, Futrell JW, Katz AJ, Benhaim P, Lorenz HP, Hedrick MH: Human adipose tissue is a source of multipotent stem cells. Mol Biol Cell 2002, 13:4279–4295
24. Kim HK, Kim JH, Abbas AA, Kim DO, Park SJ, Chung JY, Song EK, Yoon TR: Red light of 647 nm enhances osteogenic differentiation in mesenchymal stem cells. Lasers Med Sci 2009, 24:214–222
25. Steemers FJ, Chang W, Lee G, Barker DL, Shen R, Gunderson KL: Whole-genome genotyping with the single-base extension assay. Nat Methods 2006, 3:31–33
26. Benjamini Y, Hochberg Y: Controlling the false discovery rate: a practical and powerful approach to multiple testing. J R Stat Soc 1995, B57:289–300
27. Smyth GK: Limma: linear models for microarray data. Bioinformatics and Computational Biology Solutions Using R and Bioconductor. Edited by R Gentleman, V Carey, S Dudoit, R Irizarry, W Huber. New York, Springer, 2005, pp. 397–420
28. Falcon S, Gentleman R: Using GOstats to test gene lists for GO term association. Bioinformatics 2007, 23:257–258
29. Dominici M, Le Blanc K, Mueller I, Slaper-Cortenbach I, Marini F, Krause D, Deans R, Keating A, Prockop DJ, Horwitz E: Minimal criteria for defining multipotent mesenchymal stromal cells: the International Society for Cellular Therapy position statement. Cytotherapy 2006, 8:315–317
30. Kovacevic A, Hammer A, Stadelmeyer E, Windischhofer W, Sundl M, Ray A, Schweighofer N, Friedl G, Windhager R, Sattler W, Malle E: Expression of serum amyloid A transcripts in human bone tissues, differentiated osteoblast-like stem cells and human osteosarcoma cell lines. J Cell Biochem 2008, 103:994–1004
31. Sajnani-Perez G, Chilton JK, Aricescu AR, Haj F, Stoker AW: Isoform-specific binding of the tyrosine phosphatase PTPsigma to a ligand in developing muscle. Mol Cell Neurosci 2003, 22:37–48
32. Unhavaithaya Y, Hao Y, Beyret E, Yin H, Kuramochi-Miyagawa S, Nakano T, Lin H: MILI, a PIWI-interacting RNA-binding protein, is required for germ line stem cell self-renewal and appears to positively regulate translation. J Biol Chem 2009, 284:6507–6519
33. Faulk C, Dolinoy DC: Timing is everything: the when and how of environmentally induced changes in the epigenome of animals. Epigenetics 2011, 6:791–797
34. Kehat I, Kenyagin-Karsenti D, Snir M, Segev H, Amit M, Gepstein A, Livne E, Binah O, Itskovitz-Eldor J, Gepstein L: Human embryonic stem cells can differentiate into myocytes with structural and functional properties of cardiomyocytes. J Clin Invest 2001, 108:407–414
35. Collas P: Epigenetic states in stem cells. Biochim Biophys Acta 2009, 1790:900–905
36. Prockop DJ, Olson SD: Clinical trials with adult stem/progenitor cells for tissue repair: let's not overlook some essential precautions. Blood 2007, 109:3147–3151
37. Ben-David U, Mayshar Y, Benvenisty N: Large-scale analysis reveals acquisition of lineage-specific chromosomal aberrations in human adult stem cells. Cell Stem Cell 2011, 9:97–102
38. Jeong JO, Han JW, Kim JM, Cho HJ, Park C, Lee N, Kim DW, Yoon YS: Malignant tumor formation after transplantation of short-term cultured bone marrow mesenchymal stem cells in experimental myocardial infarction and diabetic neuropathy. Circ Res 2011, 108:1340–1347
39. Lazennec G, Jorgensen C: Concise review: adult multipotent stromal cells and cancer: risk or benefit? Stem Cells 2008, 26:1387–1394
40. Anisimov SV, Morizane A, Correia AS: Risks and mechanisms of oncological disease following stem cell transplantation. Stem Cell Rev 2010, 6:411–424
41. Meissner A, Mikkelsen TS, Gu H, Wernig M, Hanna J, Sivachenko A, Zhang X, Bernstein BE, Nusbaum C, Jaffe DB, Gnirke A, Jaenisch R, Lander ES: Genome-scale DNA methylation maps of pluripotent and differentiated cells. Nature 2008, 454:766–770
42. Hawkins RD, Hon GC, Lee LK, Ngo Q, Lister R, Pelizzola M, Edsall LE, Kuan S, Luu Y, Klugman S, Antosiewicz-Bourget J, Ye Z, Espinoza C, Agarwahl S, Shen L, Ruotti V, Wang W, Stewart R, Thomson JA, Ecker JR, Ren B: Distinct epigenomic landscapes of pluripotent and lineage-committed human cells. Cell Stem Cell 2010, 6:479–491
43. Ohnishi Y, Totoki Y, Toyoda A, Watanabe T, Yamamoto Y, Tokunaga K, Sakaki Y, Sasaki H, Hohjoh H: Small RNA class transition from siRNA/piRNA to miRNA during pre-implantation mouse development. Nucleic Acids Res 2010, 38:5141–5151
44. Senti KA, Brennecke J: The piRNA pathway: a fly's perspective on the guardian of the genome. Trends Genet 2010, 26:499–509
45. Kuramochi-Miyagawa S, Kimura T, Ijiri TW, Isobe T, Asada N, Fujita Y, Ikawa M, Iwai N, Okabe M, Deng W, Lin H, Matsuda Y, Nakano T: Mili, a mammalian member of piwi family gene, is essential for spermatogenesis. Development 2004, 131:839–849
46. Lee JH, Engel W, Nayernia K: Stem cell protein Piwil2 modulates expression of murine spermatogonial stem cell expressed genes. Mol Reprod Dev 2006, 73:173–179
47. Aravin AA, Sachidanandam R, Bourc'his D, Schaefer C, Pezic D, Toth KF, Bestor T, Hannon GJ: A piRNA pathway primed by individual transposons is linked to de novo DNA methylation in mice. Mol Cell 2008, 31:785–799
48. Christophersen NS, Helin K: Epigenetic control of embryonic stem cell fate. J Exp Med 2010, 207:2287–2295
49. Kirkham DL, Pacey LK, Axford MM, Siu R, Rotin D, Doering LC: Neural stem cells from protein tyrosine phosphatase sigma knockout mice generate an altered neuronal phenotype in culture. BMC Neurosci 2006, 7:50
50. Uetani N, Chagnon MJ, Kennedy TE, Iwakura Y, Tremblay ML: Mammalian motoneuron axon targeting requires receptor protein tyrosine phosphatases sigma and delta. J Neurosci 2006, 26:5872–5880
51. Imamura T, Ohgane J, Ito S, Ogawa T, Hattori N, Tanaka S, Shiota K: CpG island of rat sphingosine kinase-1 gene: tissue-dependent DNA methylation status and multiple alternative first exons. Genomics 2001, 76:117–125
52. Futscher BW, Oshiro MM, Wozniak RJ, Holtan N, Hanigan CL, Duan H, Domann FE: Role for DNA methylation in the control of cell type specific maspin expression. Nat Genet 2002, 31:175–179
53. Rauch TA, Wu X, Zhong X, Riggs AD, Pfeifer GP: A human B cell methylome at 100-base pair resolution. Proc Natl Acad Sci U S A 2009, 106:671–678
54. Grunau C, Hindermann W, Rosenthal A: Large-scale methylation analysis of human genomic DNA reveals tissue-specific differences between the methylation profiles of genes and pseudogenes. Hum Mol Genet 2000, 9:2651–2663
55. Song F, Smith JF, Kimura MT, Morrow AD, Matsuyama T, Nagase H, Held WA: Association of tissue-specific differentially methylated regions (TDMs) with differential gene expression. Proc Natl Acad Sci U S A 2005, 102:3336–3341
56. Irizarry RA, Ladd-Acosta C, Wen B, Wu Z, Montano C, Onyango P, Cui H, Gabo K, Rongione M, Webster M, Ji H, Potash JB, Sabunciyan S, Feinberg AP: The human colon cancer methylome shows similar hypo- and hypermethylation at conserved tissue-specific CpG island shores. Nat Genet 2009, 41:178–186
57. Fan Z, Yamaza T, Lee JS, Yu J, Wang S, Fan G, Shi S, Wang CY: BCOR regulates mesenchymal stem cell function by epigenetic mechanisms. Nat Cell Biol 2009, 11:1002–1009

58. Deng J, Shoemaker R, Xie B, Gore A, LeProust EM, Antosiewicz-Bourget J, Egli D, Maherali N, Park IH, Yu J, Daley GQ, Eggan K, Hochedlinger K, Thomson J, Wang W, Gao Y, Zhang K: Targeted bisulfite sequencing reveals changes in DNA methylation associated with nuclear reprogramming. Nat Biotechnol 2009, 27:353–360
59. Doi A, Park IH, Wen B, Murakami P, Aryee MJ, Irizarry R, Herb B, Ladd-Acosta C, Rho J, Loewer S, Miller J, Schlaeger T, Daley GQ, Feinberg AP: Differential methylation of tissue- and cancer-specific CpG island shores distinguishes human induced pluripotent stem cells, embryonic stem cells and fibroblasts. Nat Genet 2009, 41: 1350–1353
60. Kiskinis E, Eggan K: Progress toward the clinical application of patient-specific pluripotent stem cells. J Clin Invest 2010, 120:51–59
61. Anokye-Danso F, Trivedi CM, Juhr D, Gupta M, Cui Z, Tian Y, Zhang Y, Yang W, Gruber PJ, Epstein JA, Morrisey EE: Highly efficient miRNA-mediated reprogramming of mouse and human somatic cells to pluripotency. Cell Stem Cell 2011, 8:376–388
62. Taulli R, Bersani F, Foglizzo V, Linari A, Vigna E, Ladanyi M, Tuschl T, Ponzetto C: The muscle-specific microRNA miR-206 blocks human rhabdomyosarcoma growth in xenotransplanted mice by promoting myogenic differentiation. J Clin Invest 2009, 119:2366–2378
63. Varela C, Denis JA, Polentes J, Feyeux M, Aubert S, Champon B, Piétu G, Peschanski M, Lefort N: Recurrent genomic instability of chromosome 1q in neural derivatives of human embryonic stem cells. J Clin Invest 2012, 122:569–574
64. Tolar J, Nauta AJ, Osborn MJ, Panoskaltsis Mortari A, McElmurry RT, Bell S, Xia L, Zhou N, Riddle M, Schroeder TM, Westendorf JJ, McIvor RS, Hogendoorn PC, Szuhai K, Oseth L, Hirsch B, Yant SR, Kay MA, Peister A, Prockop DJ, Fibbe WE, Blazar BR: Sarcoma derived from cultured mesenchymal stem cells. Stem Cells 2007, 25:371–379
65. Menendez P, Catalina P, Rodríguez R, Melen GJ, Bueno C, Arriero M, García-Sánchez F, Lassaletta A, García-Sanz R, García-Castro J: Bone marrow mesenchymal stem cells from infants with MLL-AF4+ acute leukemia harbor and express the MLL-AF4 fusion gene. J Exp Med 2009, 206:3131–3141
66. Rubio R, García-Castro J, Gutiérrez-Aranda I, Paramio J, Santos M, Catalina P, Leone PE, Menendez P, Rodríguez R: Deficiency in p53 but not retinoblastoma induces the transformation of mesenchymal stem cells in vitro and initiates leiomyosarcoma in vivo. Cancer Res 2010, 70:4185–4194
67. Meza-Zepeda LA, Noer A, Dahl JA, Micci F, Myklebost O, Collas P: High-resolution analysis of genetic stability of human adipose tissue stem cells cultured to senescence. J Cell Mol Med 2008, 12:553–563
68. Dahl JA, Duggal S, Coulston N, Millar D, Melki J, Shahdadfar A, Brinchmann JE, Collas P: Genetic and epigenetic instability of human bone marrow mesenchymal stem cells expanded in autologous serum or fetal bovine serum. Int J Dev Biol 2008, 52:1033–1042
69. Berman BP, Weisenberger DJ, Laird PW: Locking in on the human methylome. Nature Biotechnol 2009, 27:341–342
70. Berdasco M, Esteller M: Aberrant epigenetic landscape in cancer: how cellular identity goes awry. Dev Cell 2010, 19:698–711